

Accepted Manuscript

Discovery of 2-oxopiperazine dengue inhibitors by scaffold morphing of a phenotypic high-throughput screening hit

Cyrille S. Kounde, Hui-Quan Yeo, Qing-Yin Wang, Kah Fei Wan, Hongping Dong, Ratna Karuna, Ina Dix, Trixie Wagner, Bin Zou, Oliver Simon, Ghislain M.C. Bonamy, Bryan K.S. Yeung, Fumiaki Yokokawa

PII: S0960-894X(17)30126-9
DOI: <http://dx.doi.org/10.1016/j.bmcl.2017.02.005>
Reference: BMCL 24677

To appear in: *Bioorganic & Medicinal Chemistry Letters*

Received Date: 10 January 2017
Revised Date: 31 January 2017
Accepted Date: 2 February 2017

Please cite this article as: Kounde, C.S., Yeo, H-Q., Wang, Q-Y., Fei Wan, K., Dong, H., Karuna, R., Dix, I., Wagner, T., Zou, B., Simon, O., Bonamy, G.M.C., Yeung, B.K.S., Yokokawa, F., Discovery of 2-oxopiperazine dengue inhibitors by scaffold morphing of a phenotypic high-throughput screening hit, *Bioorganic & Medicinal Chemistry Letters* (2017), doi: <http://dx.doi.org/10.1016/j.bmcl.2017.02.005>

This is a PDF file of an unedited manuscript that has been accepted for publication. As a service to our customers we are providing this early version of the manuscript. The manuscript will undergo copyediting, typesetting, and review of the resulting proof before it is published in its final form. Please note that during the production process errors may be discovered which could affect the content, and all legal disclaimers that apply to the journal pertain.



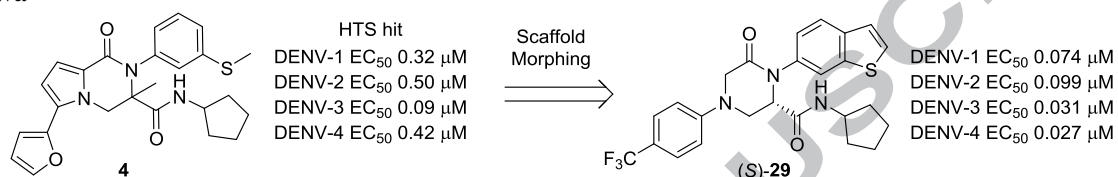
Graphical Abstract

To create your abstract, type over the instructions in the template box below.
 Fonts or abstract dimensions should not be changed or altered.

Discovery of 2-oxopiperazine dengue inhibitors by scaffold morphing of a phenotypic high-throughput screening hit

Leave this area blank for abstract info.

Cyrille S. Kounde^{a,*}, Hui-Quan Yeo^a, Qing-Yin Wang^a, Kah Fei Wan^a, Hongping Dong^a, Ratna Karuna^a, Ina Dix^b, Trixie Wagner^b, Bin Zou^a, Oliver Simon^a, Ghislain M. C. Bonamy^a, Bryan K. S. Yeung^a, and Fumiaki Yokokawa^{a,*}





Discovery of 2-oxopiperazine dengue inhibitors by scaffold morphing of a phenotypic high-throughput screening hit

Cyrille S. Kounde^{a,*}, Hui-Quan Ye^a, Qing-Yin Wang^a, Kah Fei Wan^a, Hongping Dong^a, Ratna Karuna^a, Ina Dix^b, Trixie Wagner^b, Bin Zou^a, Oliver Simon^a, Ghislain M. C. Bonamy^a, Bryan K. S. Yeung^a, and Fumiaki Yokokawa^{a,*}

^aNovartis Institute for Tropical Diseases, 10 Biopolis Road, #05-01 Chromos, Singapore 138670

^bNovartis Institute for BioMedical Research, Forum 1 Novartis Campus, CH-4056 Basel, Switzerland

ARTICLE INFO

Article history:

Received

Revised

Accepted

Available online

Keywords:

Dengue virus

NS4B

Cell-based screen

Scaffold morphing

2-Oxopiperazine

ABSTRACT

A series of 2-oxopiperazine derivatives were designed from the pyrrolo-piperazinone cell-based screening hit **4** as a dengue virus inhibitor. Systematic investigation of the structure-activity relationship (SAR) around the piperazinone ring led to the identification of compound (*S*)-**29**, which exhibited potent anti-dengue activity in the cell-based assay across all four dengue serotypes with $EC_{50} < 0.1 \mu\text{M}$. Cross-resistant analysis confirmed that the virus NS4B protein remained the target of the new oxopiperazine analogs obtained via scaffold morphing from the HTS hit **4**.

2009 Elsevier Ltd. All rights reserved.

Dengue fever is a mosquito-borne tropical disease caused by the dengue virus (DENV). It develops into flu-like symptoms and in a small proportion of cases (less than 5 %) it can lead to life-threatening dengue hemorrhagic fever (DHF) or dengue shock syndrome (DSS).¹ Dengue fever is an endemic disease in many regions of the world spreading over 100 countries and with an estimated 390 million infections each year.² The virus which is spread by mosquitoes of the *Aedes* genus is divided into four closely related but distinct serotypes (DENV 1-4); all of which are able to cause the disease. It is also known that a subsequent secondary infection with a different dengue viral serotype increases the risk factor for developing into DHF and DSS.³ Efforts towards dengue prevention have led to the approval of one dengue vaccine, although it achieved only 60 % efficacy in a phase III trial and has certain limitations (three-dose regimen needed and recommended for specific age groups).⁴ While several research groups have been pursuing antiviral drug discovery, to date, there is no drug available for the treatment of dengue fever. Therefore, there is an urgent need to develop effective and safe antiviral therapeutics to alleviate the disease burden.^{5,6}

Besides drug screening for inhibitors of viral enzymes, cell-based screening has become a powerful approach to discover chemical starting points for the development of antiviral agents such as hepatitis C virus (HCV) NS4B and NS5A inhibitors.^{7,8} As a part of our research activities for anti-dengue drug discovery, we conducted a cell-based high-throughput screening (HTS) on

the Novartis corporate compound collection using a luciferase-based replicon of DENV-2 in A549 cells. An aminothiazole **1** was identified as a pan-serotypic active hit with EC_{50} values ranging from 1.0 to 4.1 μM . However a subsequent medicinal chemistry efforts could not improve the potency.⁹ Another scaffold, a spiro-pyrazolopyridone **2** was also identified from the HTS, and optimization of its physicochemical properties led to compound **3**, which demonstrated oral *in vivo* efficacy in a DENV-2/AG129 mouse model.¹⁰ Nevertheless, this class of compounds lacked potency against DENV-1 and -4 ($EC_{50} > 20 \mu\text{M}$), despite being very active against DENV-2 and -3 (EC_{50} 0.01 to 0.08 μM). Resistance analysis showed that mutations in the dengue viral NS4B sequence (nonenzymatic transmembrane protein and a component of the viral replication complex) conferred resistance to compounds **1** and **2**, suggesting that both scaffolds from the cell-based HTS target the NS4B protein.^{9,11-13}

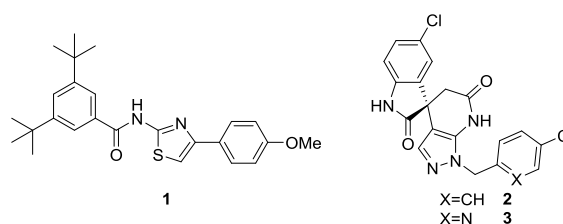


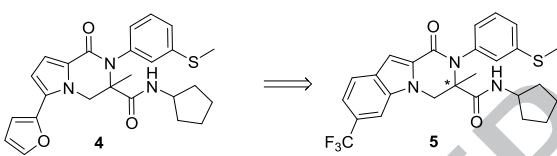
Figure 1. Reported dengue NS4B inhibitors from cell-based HTS.

In order to identify other potent and pan-serotypic chemotypes, we undertook a HTS using a cytopathic effect (CPE)-based assay in DENV-2 infected Huh-7 cell lines as a primary screen. Active compounds ($EC_{50} < 5 \mu\text{M}$) were followed up by testing for activity against all four serotypes in a DENV infected A549 cell-based flavivirus immunodetection (CFI) assay using a high content imaging readout. This led to the identification of a pyrrolpiperazinone scaffold **4** which was selected for further optimization because of its sub-micromolar activity on DENV 1-4 and low cytotoxicity ($CC_{50} > 50 \mu\text{M}$) in HepG2 cell lines (Table 1). Generation of resistant mutants led to a mutation in the viral NS4B sequence as reported for the two aforementioned scaffolds (data not shown).¹⁴ Herein, we wish to report our research towards the discovery of a 2-oxopiperazine dengue inhibitor obtained by scaffold morphing from the pyrrolpiperazinone hit **4**.

The initial hit expansion revealed that the phenylthioether and the amide groups were required for antiviral activity. Further derivatization led to the indolopiperazinone **5**, which showed a 2-4 fold improvement in potency. After a chiral separation, each enantiomer of compound **5** was profiled separately. A marked difference in EC_{50} values was observed between the pair, highlighting the importance of the chiral center (Table 1). The absolute stereochemistry of the active enantiomer was assigned as (*S*)-configuration determined by X-ray crystallographic analysis ((*S*)-**5** CCDC: 1523973).

Table 1.

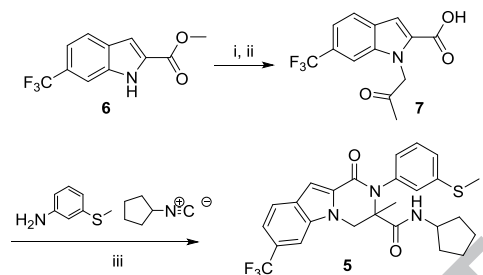
Antiviral activity of compound **4** and compound **5**



Assays (μM)	4	5	(<i>S</i>)- 5	(<i>R</i>)- 5
DENV-1 EC_{50} ^a	0.32	0.08	0.04	5.5
DENV-2 EC_{50} ^a	0.50	0.20	0.09	5.1
DENV-3 EC_{50} ^a	0.09	0.05	0.01	0.6
DENV-4 EC_{50} ^a	0.42	0.17	0.05	1.5
HepG2 CC_{50}	>50	>50	20	20

^a EC_{50} was measured in an A549 cell-based flavivirus immunodetection (CFI) assay.

Although the potency of compounds **4** and **5** on DENV1-4 was very compelling, both compounds suffered from low aqueous solubility and metabolic stability. Thus, further modifications were required and triggered an optimization campaign. However the chemical route to access the indolopiperazinone core involved a low-yielding three component Ugi-type reaction between an *N*-substituted-2-indolecarboxylic acid, an aniline and an isocyanide (Scheme 1). Structure-activity relationship (SAR) investigation towards the aminocyclopentyl group was also limited by a lack of diverse and commercially available isocyanides. We also wanted to move away from the highly rigid tricyclic system. Therefore, we envisioned a scaffold morphing approach to introduce more flexibility into the molecule by breaking certain bonds while retaining the key pharmacophore.



Scheme 1. Synthetic route of compound **5** via Ugi-type reaction. Reactions conditions: (i) bromoacetone, NaH, DMF; (ii) LiOH, *aq.* THF-MeOH; (iii) MeOH, 50°C.

In our initial attempt to increase the flexibility of the molecule, cleavage of the three bonds (a, b and c) led to the substituted indolecarboxamide derivatives **8-11** (Figure 2). All the compounds synthesized retained low micromolar antiviral activity on DENV 1-4 (Table 2). However, we concluded that the increased cytotoxicity on HepG2 cell lines was driving the cellular activity which implied that NS4B was no longer the target. This was later confirmed for compound **8** which showed no shift in EC_{50} when tested on a DENV-2 resistant mutant raised from compound **4**. Subsequently, the scaffold was altered by breaking the indole core (bond d) leading to 2-oxopiperazine analogs. The first prototype **12** was made via the same Ugi reaction that allowed the formation of a quaternary center. Unlike the other morphings, compound **12** had a good cytotoxicity window while maintaining single digit micromolar potency on 3 out of four serotypes (Table 2).

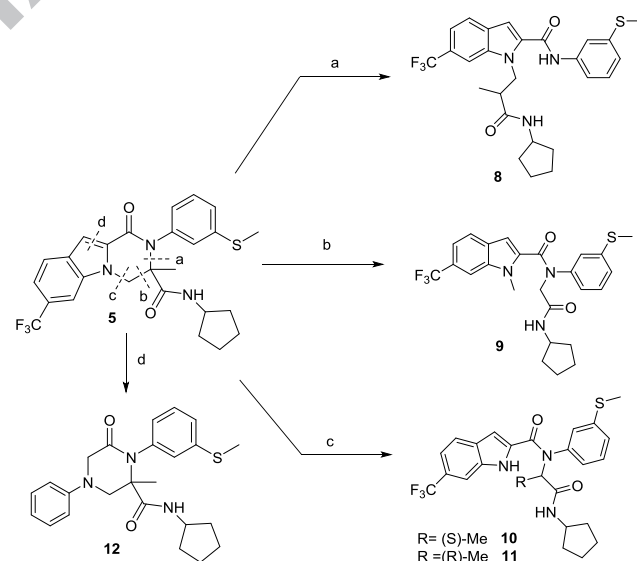


Figure 2. Compounds synthesized following the ring opening strategy (bond breaks at a, b, c, d).

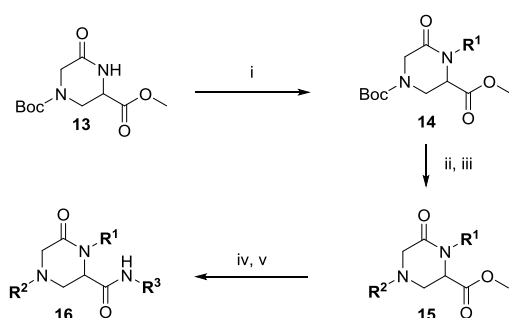
Table 2.

Antiviral activity of compounds **8-12**.

Assays (μM)	8	9	10	11	12
DENV-1 EC_{50} ^a	5.1	3.1	2.2	5.3	4
DENV-2 EC_{50} ^a	10	3	1.7	3.6	11
DENV-3 EC_{50} ^a	3.9	2.3	2	2.5	1.3
DENV-4 EC_{50} ^a	2	1.5	1.5	2.6	2.5
HepG2 CC_{50}	7.1	6.3	7.1	15	>50

^a EC_{50} was measured in an A549 cell-based flavivirus immunodetection (CFI) assay.

Encouraged by compound **12**, we re-investigated the chemical route of 2-oxopiperazine scaffold in order to expand the SAR more broadly. A five-step synthesis starting from the Boc-protected oxopiperazine **13**¹⁵ was devised (Scheme 2). *N*-arylation of the oxopiperazine **13** was achieved by copper-mediated coupling with the corresponding aryl halides in the presence of a diamine ligand and cesium carbonate as a base.¹⁶ The following steps, namely Boc-deprotection, Buchwald coupling¹⁷, hydrolysis and final amide coupling proceeded without any major hurdles. Compound **17** was prepared through this new synthetic route which also gave the opportunity to assess the effect of the methyl group at the quaternary center. Compounds **12** and **17** showed similar antiviral activity across the four serotypes, suggesting that the methyl group was not essential for activity. Up until this point we elected to work with racemates as we could always isolate the more active enantiomer (Table 3).



Scheme 2. Synthetic route to access new oxopiperazinones analogues. Reaction conditions: (i) R¹-X, CuI, *N*,*N*'-dimethylethane-1,2-diamine, Cs₂CO₃, dioxane; (ii) HCl-EtOAc; (iii) R²-X, Pd₂dba₃, DavePhos, Cs₂CO₃, dioxane; (iv) LiOH, *aq.* THF-MeOH; (v) R³-NH₂, HATU, Et₃N, DMF.

Table 3. R₂ modifications and antiviral activity.

Assays (μM)	17	18	19	20	21	22	23	24
DENV-1 EC ₅₀ ^a	2	0.5	0.7	6.1	2.9	4.1	>50	>50
DENV-2 EC ₅₀ ^a	11	0.6	1	8	5.4	7.4	>50	>50
DENV-3 EC ₅₀ ^a	0.8	0.2	0.3	6.5	1.6	1.7	13	31
DENV-4 EC ₅₀ ^a	2	0.2	0.6	5.8	2.4	2.5	28	45
HepG2 CC ₅₀	>50	10	20	10	>50	>50	>50	>50

^aEC₅₀ was measured in an A549 cell-based flavivirus immunodetection (CFI) assay.

The des-methyl oxopiperazine core did not only simplify the scaffold and the chemical route, but it also allowed access to expand the SAR at the R³ position which was limited with scaffold **12** (Scheme 2). Our exploration started with the phenyl group (R² modifications) while keeping in place the phenylthioether (R¹) and the cyclopentylamine (R³) moieties. Buchwald *N*-arylation was used to install various substituted phenyls at R². The *para* trifluoromethyl group (*p*-CF₃, **18**) gave a 4-10 fold improvement in activity as compared with compound **17**. The *meta* or *para* orientation of the -CF₃ did not have an influence on the antiviral activity as shown by compound **19** (*m*-CF₃). It is noteworthy that the EC₅₀ values of both **18** and **19** were markedly shifted to more than 10-fold higher in the resistant virus generated by compound **4**, suggesting that the oxopiperazines derived from the pyrrolo-piperazinone also worked through inhibiting the NS4B protein (data not shown).¹⁴ Incorporating an additional methyl on the benzene ring of **19** led to a 10-fold loss in activity (compound **20**). Electron donating group such as the methoxy group (-OMe, **21**) also resulted in a 5-fold loss. Polar substitutions were not tolerated as shown by the activity data for the cyanophenyl group (compound **22**) and the pyridyl group (compound **23** and **24**) (Table 3).

We then turned to the R¹ position where the phenylthioether was replaced with simple substituted aryl groups as well as bicyclic systems (Table 4). Switching the phenylthioether of **19** for a pyridylthioether gave the equipotent analogue **25**. Interestingly, we also observed a 10-fold improvement in solubility through this replacement (solubility at pH 6.8 = 4 μM for **19**, 40 μM for **25**). Thioether isosteres have been looked at and the derivatives **26-28** were synthesized. While the trifluoromethoxy group (-OCF₃) and the difluoromethyl (-CF₂CH₃) were tolerated (**27**, **28** respectively but with lower CC₅₀ values), the methylketone **26** suffered a 10-fold loss of potency across the four serotypes. Another strategy targeting the thioether involved a ring closure to form the benzothiophene **29**. Pleasingly, **29** showed the best potency observed in this new oxopiperazine series. Chiral separation was conducted to purify the enantiomers (*S*)-**29** and (*R*)-**29** and the stereochemistry was confirmed by X-ray crystallography. Compound (*S*)-**29** had an antiviral activity matching the same stereochemistry of indolopiperazinone (*S*)-**5** ((*S*)-**29** CCDC: 1523972). As for the benzofuran **30** and the thienopyridine **31**, they both suffered a 4-fold loss as compared with **29**.

Having incorporated optimized moieties for R¹ and R², we scaled up a key building block which enabled a screen of R³ (Figure 3). Considering the breakthrough obtained with the benzothiophene introduction, it was decided to keep it as R¹ while R² was maintained as a phenyl group for easier comparison with the analogue **17**.

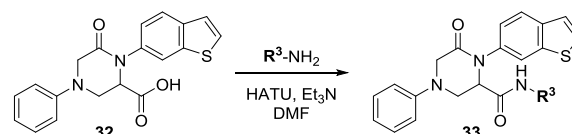
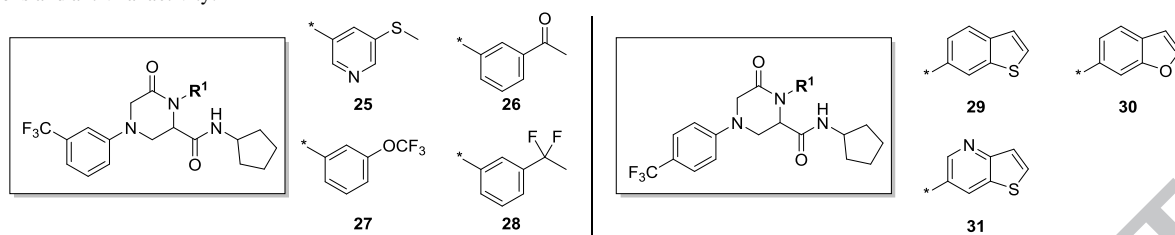


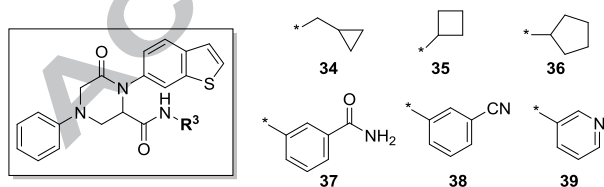
Figure 3. Building block **32** chosen for library synthesis.

Table 4.R¹ modifications and antiviral activity.

Assays (μM)	25	26	27	28	29	(S)-29	(R)-29	30	31
DENV-1 EC ₅₀ ^a	0.4	7.1	1.1	1.9	0.2	0.07	6.9	0.8	0.5
DENV-2 EC ₅₀ ^a	1.2	10	1.7	2.2	0.3	0.1	5.7	1	0.9
DENV-3 EC ₅₀ ^a	0.2	2.2	0.4	0.4	0.08	0.03	2.6	0.4	0.3
DENV-4 EC ₅₀ ^a	0.6	6.3	0.7	0.8	0.1	0.03	2.6	0.5	0.4
HepG2 CC ₅₀	26	40	8	9	10	20	10	20	30

^aEC₅₀ was measured in an A549 cell-based flavivirus immunodetection (CFI) assay.

A selection of various amines (aliphatic, aromatic, primary and secondary amines) was included in the library design and a total of 44 compounds was synthesized. We report here only a selection of the most active analogs obtained. In summary, the amide nitrogen -NH proved to be important as all tertiary amides were completely inactive. Similarly, additional basic centers (primary or secondary amines) as well as free hydroxyl groups were not tolerated (data not shown). Small aliphatic groups emerged as the most preferred as suggested by the antiviral activity of **34** (methylcyclopropyl), **35** (cyclobutyl), and **36** (cyclopentyl). Finally, substituted phenyl with polar groups **37** and **38** along with the pyridyl **39** were some of the few compounds that maintained single digit micromolar potency across dengue serotypes. The library approach was an efficient way of probing R³. However, none of the substitutions showed superiority over the initial cyclopentyl **36** apart from the cyclobutyl **35** (Table 5). With the trifluoromethyl group (-CF₃) preferred on the phenyl from R² and the benzothiophene preferred on R¹, compound **29** and (S)-**29** proved to be unequalled.

Table 5.Selected R³ modifications and antiviral activity.

Assays (μM)	34	35	36	37	38	39
DENV-1 EC ₅₀ ^a	6.2	1.8	2.4	2	2.8	5.6
DENV-2 EC ₅₀ ^a	2.2	1	1.5	1.5	2	2.7
DENV-3 EC ₅₀ ^a	0.2	0.05	0.17	0.13	0.09	0.5
DENV-4 EC ₅₀ ^a	0.6	0.2	0.9	1.9	1.2	1.7
HepG2 CC ₅₀ ^a	>50	>50	>50	>50	>50	>50

^aEC₅₀ was measured in an A549 cell-based flavivirus immunodetection (CFI) assay.

In vitro profiling of (S)-**29** was also conducted and compared with the indolopiperazinone (S)-**5**. Although the solubility was not impacted, a 10-fold improvement in human microsomal metabolic stability was achieved (Table 6).

Table 6.*In vitro* profile of compound (S)-**5** and (S)-**29**.

Assays	(S)- 5	(S)- 29
Solubility at pH 6.8 (μM)	<4	<4
Human CL _{int} ($\mu\text{L}/\text{min}/\text{mg}$) ^a	>735	59
LogD (pH 7.4)	>4.5	>4.5

^a Measured in human liver microsomes.

In conclusion, starting from the rigid pyrrolo-piperazinone hit **4** with a sub-micromolar activity on DENV 1-4, we applied a scaffold morphing approach that led to the easily accessible oxopiperazine core. Although the optimized chemical route enabled efficient scaffold derivatization and led to a potent pan-serotypic oxopiperazine analog (S)-**29**, the series could not be further progressed due to its unfavorable physicochemical properties (low solubility, high lipophilicity). Despite the outcome, this research emphasized the usefulness of a scaffold morphing approach to complement a cell-based screen.

Acknowledgments

We thank the following colleagues from Novartis who participated in generating the data presented in this paper: Katherine Chan, Chin Chin Lim, Hao Ying Xu, Boon Heng Lee, Jeremy Selva, Ivan Low, Ai Ping Hiu, Joefina Lim, and Prakash Vachaspati.

We also thank Dr. Joseph Shambabu Maddirala and his colleagues in GVK Biosciences and Dr. Feng Zhao and his colleagues in WuXi App Tec. for their technical assistance.

We are grateful to Dr. Jürgen Wagner for his critical reading of the manuscript.

Supplementary data

Supplementary data (synthetic procedures, spectral characterization and the antiviral assays) associated with this article can be found, in the online version, at <http://> --

References and notes

- Whitehorn, J.; Simmons, C. P. *Vaccine* **2011**, *29*, 7211.
- Bhatt, S.; Gething, P. W.; Brady, O. J.; Messina, J. P.; Farlow, A. W.; Moyes, C. L.; Drake, J. M.; Brownstein, J. S.; Hoen, A. G.; Sankoh, O.; Myers, M. F.; George, D. B.; Jaenisch, T.; Wint, G. R. W.; Simmons, C. P.; Scott, T. W.; Farrar, J. J.; Hay, S. I. *Nature* **2013**, *496*, 504.
- Guzman, M. G.; Alvarez, M.; Halstead, S. B. *Arch. Virol.* **2013**, *158*, 1445.
- Capeding, M. R.; Tran, N. H.; Hadinegoro, S. R.; Ismail, H. I.; Chotpitayasunondh, T.; Chua, M. N.; Luong, C. Q.; Rusmil, K.; Wirawan, D. N.; Nallusamy, R.; Pitisuttithum, P.; Thisyakorn, U.; Yoon, I.-K.; van der Vliet, D.; Langevin, E.; Laot, T.; Hutagalung, Y.; Frago, C.; Boaz, M.; Wartel, T. A.; Tornieporth, N. G.; Saville, M.; Bouckennooghe, A. *Lancet* **2014**, *384*, 1358.
- Lim, S. P.; Wang, Q.-Y.; Noble, C. G.; Chen, Y.-L.; Dong, H.; Zou, B.; Yokokawa, F.; Nilar, S.; Smith, P.; Beer, D.; Lescar, J.; Shi, P.-Y. *Antivir. Res.* **2013**, *100*, 500.
- Behnam, M. A. M.; Nitsche, C.; Boldescu, V.; Klein, C. D. *J. Med. Chem.* **2016**, *59*, 5622.
- Cannalire, R.; Barreca, M. L.; Manfroni, G.; Cecchetti, V. *J. Med. Chem.* **2016**, *59*, 16.
- Belema, M.; Lopez, O. D.; Bender, J. A.; Romine, J. L.; St. Laurent, D. R.; Langley, D. R.; Lemm, J. A.; O'Boyle, II, D. R.; Sun, J.-H.; Wang, C.; Fridell, R. A.; Meanwell, N. A. *J. Med. Chem.* **2014**, *57*, 1643.
- Xie, X.; Wang, Q.-Y.; Xu, H. Y.; Qing, M.; Kramer, L.; Yuan, Z.; Shi, P.-Y. *J. Virol.* **2011**, *85*, 11183.
- Zou, B.; Chan, W. L.; Ding, M.; Leong, S. Y.; Nilar, S.; Seah, P. G.; Liu, W.; Karuna, R.; Blasco, F.; Yip, A.; Chao, A.; Susila, A.; Dong, H.; Wang, Q. Y.; Xu, H. Y.; Chan, K.; Wan, K. F.; Gu, F.; Diagana, T. T.; Wagner, T.; Dix, I.; Shi, P.-Y.; Smith, P. W. *ACS Med. Chem. Lett.* **2015**, *6*, 344.
- Wang, Q. Y.; Dong, H.; Zou, B.; Karuna, R.; Wan, K. F.; Zou, J.; Susila, A.; Yip, A.; Shan, C.; Yeo, K. L.; Xu, H.; Ding, M.; Chan, W. L.; Gu, F.; Seah, P. G.; Liu, W.; Lakshminarayana, S. B.; Kang, C.; Lescar, J.; Blasco, F.; Smith, P. W.; Shi, P.-Y. *J. Virol.* **2015**, *89*, 8233.
- Xie, X.; Zhou, J.; Wang, Q.-Y.; Shi, P.-Y. *Antivir. Res.* **2015**, *118*, 39.
- Zmurko, J.; Neyts, J.; Dallmeier, K. *Rev. Med. Virol.* **2015**, *25*, 205.
- Our preliminary data generated for compound **4** point towards a mutation located at a different position in NS4B from compounds **1** and **2**. Further analysis is currently underway.
- Itoh, F.; Hosono, H.; Kawamura, M.; Kobo, K. WO200007847.
- Ghinet, A.; Oudir, S.; Henichart, J.-P.; Rigo, B.; Pommery, N.; Gautret, P. *Tetrahedron* **2010**, *66*, 215.
- Ruiz-Castillo, P.; Buchwald, S. L. *Chem. Rev.* **2016**, *116*, 12564.

Click here to remove instruction text...